Thermally-Induced Vibration Control of Rotating Composite Thin-Walled Blade

Hoedo Jung, Sungsoo Na , Munkyu Kwak and Seok Heo

회전하는 복합재 블레이드의 열진동 해석 및 제어

정회도† · 나성수* · 곽문규** · 허석***

Key Words : rotating thin-walled blade(회전하는 박판 블레이드), smart composite material(지능복합재료), velocity feedback control(속도 되먹임 제어), displacement feedback control(변위 되먹임 제어), thermally-induced vibration(열진동)

Abstract

This paper deals with a vibration control analysis of a rotating composite blade, modeled as a tapered thin-walled beam induced by heat flux. The displayed results reveal that the thermally induced vibration yields a detrimental repercussions upon their dynamic responses. The blade consists of host graphite epoxy laminate with surface and spanwise distributed transversely isotropic (PZT-4) sensors and actuators. The controller is implemented via the negative velocity and displacement feedback control methodology, which prove to overcome the deleterious effect associated with the thermally induced vibration. The structure is modeled as a composite thin-walled beam incorporating a number of nonclassical features such as transverse shear, secondary warping, anisotropy of constituent materials, and rotary inertias.

1. Introduction

The increasing use of fiber-reinforced, composite, thin-walled beam construction for rotor blades used in helicopter, tilt rotor aircraft, turbo engine and other applications, has generated a great deal of research activity aimed at enhancing their dynamic response performances. For reasons of efficiency involving gas dynamics and weight, they must be thin, yet to operate in severe thermal environments and at higher rotational speeds. Both the dynamic equations involving the temperature effects and the related boundary conditions are obtained via the application of Hamilton's variational principle. In its modeling the effects of anisotropy of constituent materials, transverse shear, warping, rotatory inertia, etc are incorporated. In addition, in order to induce elastic couplings between flapwise bending and chordwise bending, a special ply-angle distribution achieved via the usual helically wounding fiber-reinforced technology is implemented. The numerical simulations display deflection time-history as a function of the fiber orientation of the composite materials, rotating speed, taper ratio as well as control efficiency.

Boley[1] was the first to include inertia effects in calculating the thermal-structural response of a beam subject to rapid heating and presented the governing equations for the problem of thermally induced vibrations. Seibert and Rice[2] investigated coupled thermoelastic effect for Euler-Bernoulli and Timoshenko beam model. Johnston and Thornton[3] analyzed the effects of thermally induced structural disturbances of an appendage on the dynamics of a simple spacecraft. Numerical results showed that the system dynamic response consisted of a slowly developed pointing error and superimposed oscillations, whose magnitude was related to the ratio of the thermal and structural response times of the appendage.

The coupled thermal-structural analysis that includes the effects of structural deformations on heating and temperature gradients is used to investigate the unstable motion. Thornton and Kim[4] developed an analytical approach to determine the thermal-structural response of a flexible rolled-up solar array due to a sudden increase in the external heating. The coupled

† Graduate Student, Korea University
E-mail : mydas94@korea.ac.kr
TEL : (02)3290-3854
* Assistant Professor, Korea University
** Professor, Dong-Guk University
***Postdoc, Dong-Guk University

thermal-structural analysis responses were compared with the uncoupled analysis results. I. Yoon and O. Song[5] investigated thermally induced vibration of composite thin-walled beam. The structure is modeled as a circular thin-walled beam of closed cross section and has constant cross area ratio.

Although of an evident importance, to the best of authors' knowledge, no such studies including thermal-induced vibration control of rotating composite thin-walled blade.

2. Thermal Analysis

2.1 Basic Assumption

A thin-walled beam of radius R and wall thickness is considered (Fig. 1). The blade is subjected to a known incident heat flux S applied at time t=0. The problem is to determine the transient temperature response of the tip. To this end, the following assumptions are adopted.

1. Heat is conducted only in the circumferential direction, implying that the heat conduction along the blade length is negligible,
2. Thermal energy losses at the cantilevered support at x=0 are neglected, and thermal energy is emitted from external surface of the blade assuming diffuse radiation, but internal radiation within the blade is neglected,
3. The temperature field is assumed to be uniform across the beam thickness, implying that the temperature gradient across it is neglected,
4. Convection heat transfer inside and outside the beam is negligible,

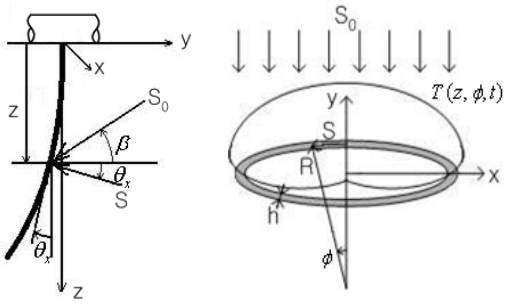

a) Heat flux b) Beam Cross section

Fig.1 Heat flux for coupled thermal-structural analysis

In such a context, the thermodynamic equation of heat conduction and radiation is

$$\frac{\partial T}{\partial t}-\frac{k}{\rho cR^2}\frac{\partial^2 T}{\partial \phi^2}+\frac{\sigma\varepsilon}{\rho ch}T^4=\frac{\alpha S_0}{\rho ch}\delta\cos\phi\cos(\beta+\theta_x) \quad (1)$$

In Eq. (1), $T\equiv(z,\phi,t)$ is the absolute temperature at an arbitrary point of beam, k is the thermal conductivity, ρ and c are the weight density and the specific heat of the material, respectively, t is time coordinate and δ is unity for the values of circumferiantial coordinate ϕ corresponding to the portion of beam surface exposed to radiation and zero otherwise. The heat flux intensity of radiation source at an angle β with respect to the direction normal to the undeflected beam axis, S_0 , is related to the counterpart one at an arbitrary point of the deflected beam surface, S, by

$$S=S_0\cos(\beta+\theta_x) \quad (2)$$

The thermodynamic equation of heat-conduction-radiation can be linearized. As a result, one can represent T as

$$T(z,\phi,t)=T_0+T_1(z,\phi,t) \quad (3)$$

where $T_1(z,\phi,t)$ is the disturbance temperature, T_0 is the steady-state absolute temperature fulfilling the condition T_0 ¨ $T_1(z,\phi,t)$.

Further, we will consider

$$T_1(z,\phi,t)=\hat{T}(z,t)\cos\phi \quad (4)$$

where $\hat{T}$ is the maximum disturbance temperature. As a result of (3), $T^4(z,\phi,t)$ intervening in Eq. (1) is expressed as a truncated binomial series expansion about T_0 in the form

$$T^4(z,\phi,t)\cong T_0^4+4T_0^3\hat{T}(z,t)\cos\phi \quad (5)$$

Moreover, the heat flux distribution on the right of Eq. (1) is represented as:

$$\delta\cos\phi=\frac{3}{2\pi}+\left(\frac{1}{2}+\frac{3\sqrt{3}}{4\pi}\right)\cos\phi \quad (6)$$

By virtue of Eqs. (5) and (6), from Eq. (1) on obtain

$$T_0=\left(\frac{3}{2\pi}\frac{\alpha S_o\cos\beta}{\sigma\varepsilon}\right)^{1/4} \quad (7)$$

and

$$\frac{\partial\hat{T}}{\partial t}+\frac{1}{\tau}\hat{T}=\frac{T^*}{\tau}\cos(\beta+\theta_x) \quad (8)$$

where

$$\frac{1}{\tau}=\frac{k}{\rho cR^2}+\frac{4\sigma\varepsilon T_0^3}{\rho ch} \quad \text{and,} \quad T^*=\left(\frac{1}{2}+\frac{3\sqrt{3}}{4\pi}\right)\frac{\sigma S_0}{\rho ch}\tau \quad (9)$$

A characteristic time and the time-independent maximum disturbance temperature when the blade is deflected statically. Assuming zero initial conditions, from Eq. (8) on obtains

$$\hat{T}(z,t)=\frac{e^{-t/\tau}T^*}{\tau}\int_0^t e^{p/t}\cos(\beta+\theta_x)dp \quad (10)$$

where p is a dummy time variable. It is readily seen that the disturbance temperature as expressed by Eq. (10) depends nonlinearly on θ_x. Assuming θ_x to be small, one can linearize

$\hat{T}(z,t)$ as to become

$$\hat{T}(z,t)=\frac{e^{-t/\tau}T^*}{\tau}\int_0^t e^{p/t}(\cos\beta-\sin\theta_x)dp \quad (11a)$$

Assuming that the beam is deflected statically, one can readily determine from (11a) the quasi-steady counterpart of $\hat{T}$

$$\hat{T}(z,t)=T^*(1-e^{-t/\tau})\cos\beta \quad (11b)$$

By virtue of (11b), $\hat{T}$ assumes a uniform behavior

in the spanwise direction.. Moreover, the steady-state counterpart of (11b) results as $\hat{T} = T^* \cos\beta$.

3. Formulation of The Composite Thin-Walled Beam Model

3.1 Basic Assumptions and Kinematics of the Modeling Formulation

The tapered composite blade consisting of a single cell thin-walled beam is mounted on a rigid hub (radius R_0) that rotates with constant angular velocity W about origin O (Fig. 2).

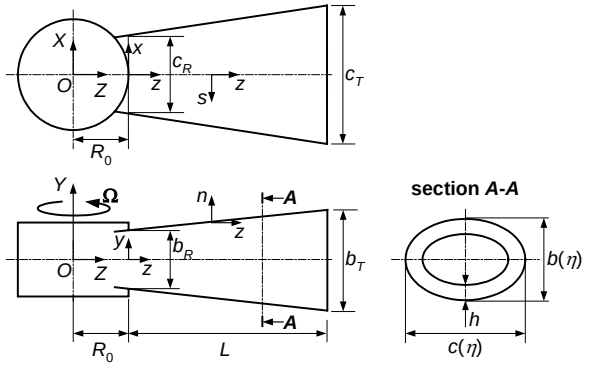

Fig.2 Geometric Configuration of the rotating blade

The inertial reference system (X, Y, Z) is attached to the center of the hub O. By (**i**, **j**, **k**) and (**I**, **J**, **K**), we define the unit vectors associated with the coordinate systems (x, y, z) and (X, Y, Z), respectively. The equations of rotating thin-walled beam are based on the following statements[6,7,8]: (i) the original cross-section of the beam is preserved; (ii) the secondary warping effects are included; (iii) transverse shear, Coriolis effect, and centrifugal acceleration are incorporated; and finally, (iv) the constituent material of the structure features thermomechanical anisotropic properties.

The linear distribution of the chord $c(\eta)$ and height $b(\eta)$ of the mid-line cross-section profiles along the beam span is considered as

$$\begin{Bmatrix} c(\eta) \\ b(\eta) \end{Bmatrix} = \left[1-\eta(1-\sigma)\right] \begin{Bmatrix} c_R \\ b_R \end{Bmatrix} \tag{12}$$

Herein $\sigma \equiv c_T / c_R$ denotes the taper ratio, $\eta \equiv z/L$ is the dimensionless spanwise coordinate, where L denotes the beam semi-span, and subscripts R and T identify its characteristics at the root and tip cross-sections, respectively. In the same context, the radius of curvature of the circular arc associated with the midline contour at section η along the beam span varies according to the relationship:

$$R(\eta) = \left[1-\eta(1-\sigma)\right] R_R \tag{13}$$

The points of the beam cross-sections are identified by the global coordinates x, y and z, where z is the spanwise coordinate and by a local one, n, s, and z, where n and s denote the thicknesswise coordinate normal to the beam mid-surface and the tangential one along the contour line of the beam cross-section, respectively. (see Fig. 2) Following coordinates description, $q_x(z,t)$ and $q_y(z,t)$ denote the rotations about axes x and y respectively, while g_{yz} and g_{xz} denote the transverse shear in the planes yz and xz respectively and the primes denote derivatives with respect to the z-coordinate. respectively

In accordance with the above assumptions and in order to reduce the 3-D problem to an equivalent 1-D, the components of the displacement vector are expressed as [6]

$$\begin{aligned} u(x,y,z,t) &= u_0 - y\phi(z,t) \\ v(x,y,z,t) &= v_0 + x\phi(z,t) \\ w(x,y,z,t) &= w_0(z,t) + \theta_x(z,t)[y(s) - n\frac{dx}{ds}] \\ &\quad + \theta_y(z,t)[x(s) + n\frac{dy}{ds}] \\ &\quad - \phi'(z,t)[F_w(s) + na(s)] \end{aligned} \tag{14}$$

$$\begin{aligned} \theta_x(z,t) &= \gamma_{yz}(z,t) - v_0'(z,t) \\ \theta_y(z,t) &= \gamma_{xz}(z,t) - u_0'(z,t) \end{aligned} \tag{15}$$

Eqs. (14) and (15) reveal that the kinematic variables, $u_0(z,t)$, $v_0(z,t)$, $w_0(z,t)$, $\theta_x(z,t)$, $\theta_y(z,t)$ and $\phi(z,t)$ representing three translations in the x, y, z directions and three rotations about the x, y, z directions, respectively are used to define the displacement components, u, v and w.

Notice that the z - axis is located as to coincide with the locus of symmetrical points of the cross-section along the wing span.

The kinetic energy K, and potential energy V, expressions for a beam are

$$\begin{aligned} K &= \frac{1}{2}\int_\tau \rho(\dot{\mathrm{R}}_i \cdot \dot{\mathrm{R}}_i) d\tau \\ V &= \frac{1}{2}\int_\tau \sigma_{ij}\varepsilon_{ij} d\tau \\ &= \frac{1}{2}\int_0^L \oint_C \sum_{k=1}^{N} \int_{h(k)} [\sigma_{bzz}\varepsilon_{bzz} + \sigma_{bsz}\gamma_{bsz} + \sigma_{bnz}\gamma_{bnz}]_{(k)} dnds dz \end{aligned} \tag{16}$$

The expressions for the virtual work done by externally applied forces are

$$\partial W_f = \int_0^L f(z,t)\delta v(z,t) dz \tag{17}$$

In these equations $d\tau(\hat{U}dndsdz)$ denotes the differential volume element and the position vector $R\hat{U}R(x,y,z,t)$ relative to a fixed origin O, of a point the deformed beam is defined as:

$$\mathrm{R} = \mathrm{R}_0 + \mathrm{r} + \Delta \tag{18}$$

In eq. (18), $r(\hat{U}xi+yj+zk)$ defines the undeformed position of a point measured in the beam coordinate system and $D(\hat{U}ui+vj+wk)$ denotes the displacement vectors of the points of the blades, while $R_0 = R_0k$.

3.2 The Equations of Motion and Boundary conditions

In order to obtain the coupled bending equations of adaptive rotating beams and the associated boundary conditions, the extended Hamilton's principle is applied.

$$\int_{t0}^{t1}(\delta K-\delta V+\delta W)dt=0$$
$$\delta u_0=\delta v_0=\delta\theta_x=\delta\theta_y=0 \quad \text{at} \quad t=t_1,t_2 \tag{19}$$

Herein K and V denote the kinetic and strain energy, respectively, δW is the virtual work of external forces, t_1 and t_2 are two arbitrary instants of time, while δ is the variational operator.

The Equations Governing the (flap-lag) Bending-Transverse Shear Motion:

$$[a_{43}\theta_x'+a_{44}(u_0'+\theta_y)]'+\Omega^2\{P(z)u_0'\}'-b_1\Omega^2u_0-b_1\ddot{u}_0-h_4^{T\prime}=0,$$
$$[a_{52}\theta_y'+a_{55}(v_0'+\theta_x)]'+\Omega^2\{P(z)v_0'\}'-b_1\ddot{v}_0-h_5^{T\prime}=0,$$
$$[a_{22}\theta_y'+a_{25}(v_0'+\theta_x)]'-a_{44}(u_0'+\theta_y)-a_{43}\theta_x'$$
$$-(b_5+b_{15})(\ddot{\theta}_y-\Omega^2\theta_y)-h_2^{T\prime}+h_4^T=0,$$
$$[a_{33}\theta_x'+a_{34}(u_0'+\theta_y)]'-a_{55}(v_0'+\theta_x)-a_{52}\theta_y'$$
$$-(b_4+b_{14})(\ddot{\theta}_x-\Omega^2\theta_x)-h_3^{T\prime}+h_5^T=0 \tag{20a-d}$$

The associated BCs for the rotating beams clamped at $z=0$ and free at $z=L$ are:

At $z=0$, $u_0=v_0=\theta_y=\theta_x=0$ (21a-d)

At $z=$L,

$$a_{43}\theta_x'+a_{44}(u_0'+\theta_y)=h_4^T,$$
$$a_{52}\theta_y'+a_{55}(v_0'+\theta_x)=h_5^T,$$
$$a_{22}\theta_y'+a_{25}(v_0'+\theta_x)=h_2^T-M_y^{a\prime},$$
$$a_{33}\theta_x'+a_{34}(u_0'+\theta_y)=h_3^T-M_x^{a\prime} \tag{22a-d}$$

In Eqs. (20) through (22), a_{ij}, b_i denote global stiffness and mass quantities, respectively. $P(z)$ is obtained as

$$P(z)=\int_z^L b_1(z)(R_0+z)\,dz \tag{23}$$

and $h_i^T(\hat{U}h_i^T(z,t))$ denote the thermal stress-resultants and thermal stress-couples defined as:

$$h_2^T=\oint_C(xN_1^T+\frac{dy}{ds}N_4^T)ds,\quad h_4^T=\oint_C N_2^T\frac{dx}{ds}ds$$
$$h_3^T=\oint_C(yN_1^T-\frac{dx}{ds}N_4^T)ds,\quad h_5^T=\oint_C N_2^T\frac{dy}{ds}ds \tag{24a-d}$$

3.3 Piezoelectric Distribution and the Control Law

For the general case, the expression of the piezoelectrically induced bending moment is given by

$$M_x^{a\prime}(z,t)=C_xV(t)[H(z-z_1)-H(z-z_2)]$$
$$M_y^{a\prime}(z,t)=C_yV(t)[H(z-z_1)-H(z-z_2)] \tag{25a,b}$$

where C_x,C_y is a constant dependent on the mechanical and geometrical properties of the piezoactuator and host structure and $V(t)$ is the applied input voltage that is equal and opposite in sign in the upper and lower piezoactuators(out-of-phase actuation). $H(\cdot)$ denotes the Heaviside function representing the actuator distribution. (Fig. 3)

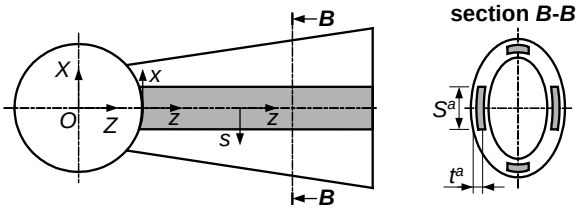

Fig. 3 Distribution of Piezoactutors

In the previously displayed equations, due to the special distribution of piezoactuators, it was shown that the piezoelectrically induced moment intervenes solely in the boundary conditions associated with the bending motion, prescribed at the beam tip, and hence it plays the role of the boundary moment control. Within the adopted feedback control law the piezoelectrically induced bending moment at the blade tip is expressed as

$$M_x^{a\prime}(L)=k_{vx}\dot{\theta}_x(L)+k_{px}\theta_x(L)$$
$$M_y^{a\prime}(L)=k_{vy}\dot{\theta}_y(L)+k_{py}\theta_y(L) \tag{26a,b}$$

Herein k_x, k_y denotes the velocity feedback gain, and in the numerical simulations nondimensional counterpart of k_x, k_y is K_x, K_y defined by

$$K_{vx}=k_{vx}L^2/a_{33}^0\quad,K_{px}=k_{px}L^2/a_{33}^0$$
$$K_{vy}=k_{vy}L^2/a_{22}^0\quad,K_{py}=k_{py}L^2/a_{22}^0 \tag{27a,b}$$

4. Numerical Simulations

A numerical study was performed to investigate the dynamic response of the system consisting of a rotating composite thin-walled blade exposed to an incident heat flux applied instantaneously at $t=0$. The data on which basis the numerical simulations have been generated are supplied in Table 1(Appendix).

Figs. 4 through 6 highlight the effects of angular velocity Ω and ply angle orientation on the natural frequencies of the coupled bending (flap-lag). The result displayed in Figs. 4 through 6 reveal the sensitivity of modal frequencies to ply angle orientation. This characteristic of composite materials provides a powerful tool in efforts to structurally tailored helicopter and tilt rotor aircraft blades for improved dynamic responses.

Figs. 7 and 8 highlight the effect of the incident angle of heat flux and of taper ratio on the dynamic response behavior. The results reveal that taper ratio plays a significant role in confining the deflection response. Fig. 9 displays the time-history of transversal and tangential

deflection response. This graph highlights the strong effect played by the angular velocity. In fig. 10 there are depictions of uncontrolled and controlled flapping response time-history of a blade subjected to heat flux.

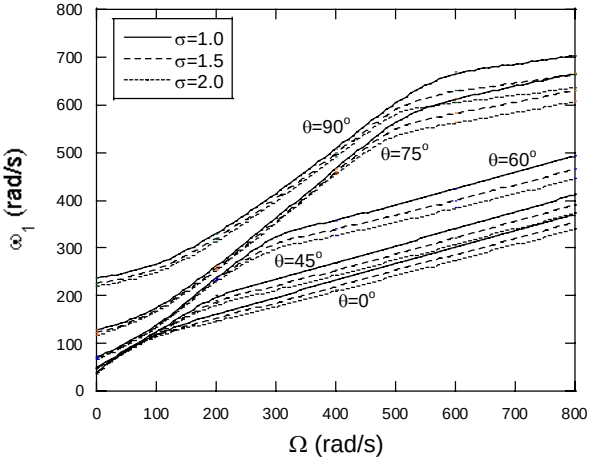

Fig. 4 First coupled flap-lag bending frequency vs. Ω for different ply angles

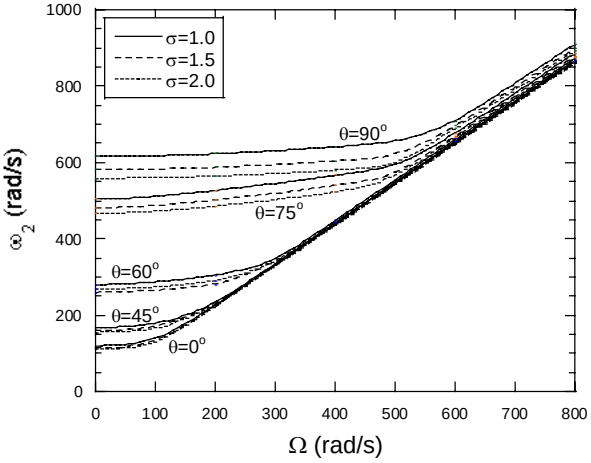

Fig. 5 Second coupled flap-lag bending frequency vs. Ω for different ply angles

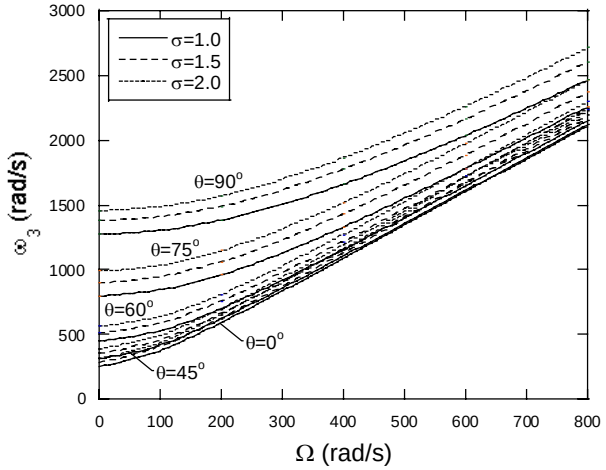

Fig. 6 Third coupled flap-lag bending frequency vs. Ω for different ply angles

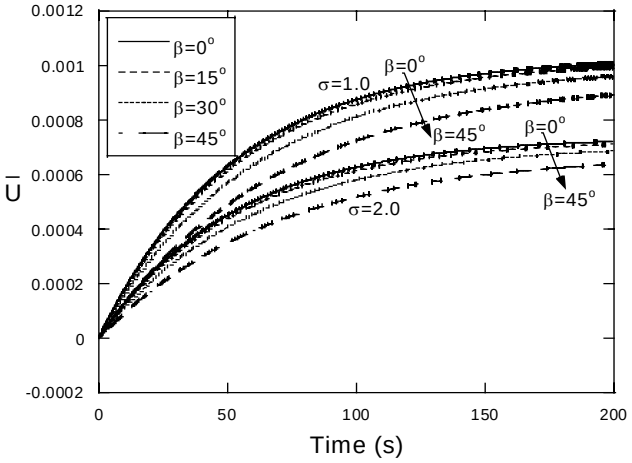

Fig. 7 Nondimensional lagging response for various heat incident angle, θ=30°, Ω=200 rad/s

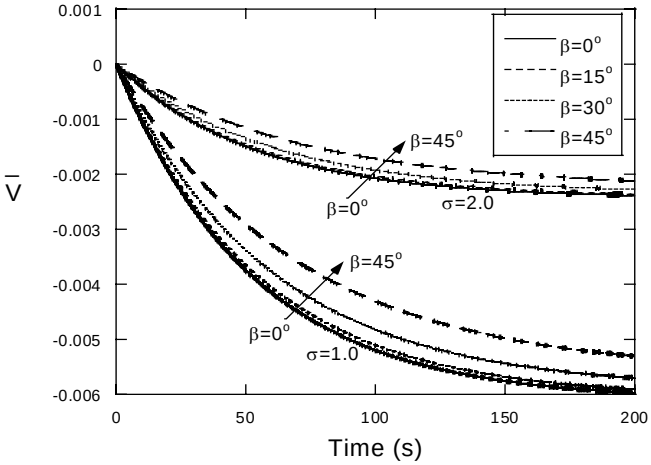

Fig. 8 Nondimensional flapping response for various heat incident angle, θ=30°, Ω=200 rad/s

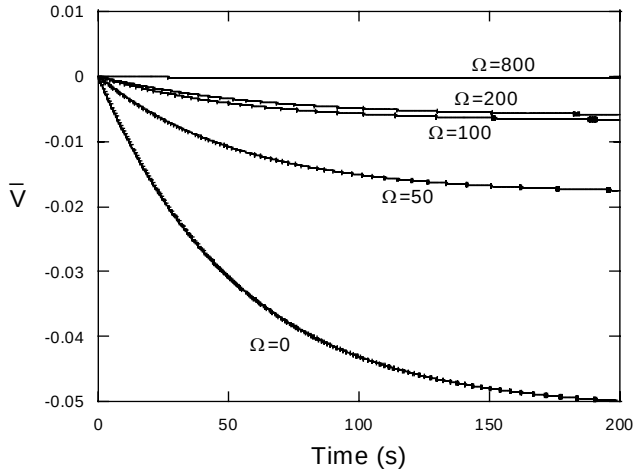

Fig. 9 Nondimensional flapping response for various angular velocity, σ=2, θ=30°, β=15°

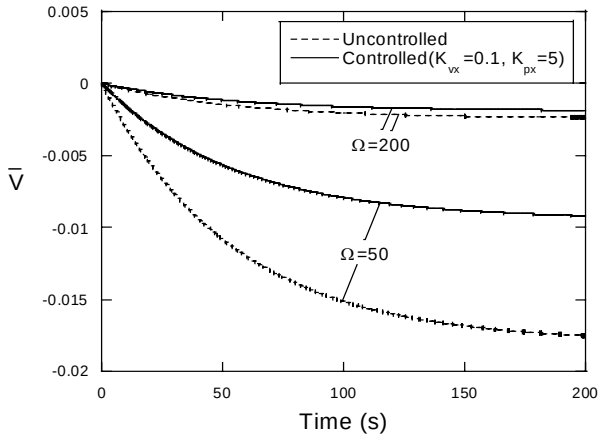

Fig. 10 uncontrolled and controlled flapping response for various angular velocity, σ=2, θ=30^{o}, β=15^{o}

5. Conclusions

A comprehensive structural model of rotating composite thin-walled blade was developed and the problem of the thermally induced vibrations was addressed.

The effects of the heat incident angle, rotating speed, blade taper ratios and ply angles of composite materials to the dynamic response of the fan blade are studied by using the coupled thermal-structural analysis. blade taper ratios and ply angles of composite materials may decrease the quasi-static and dynamic deflection of the blade.

Acknowledgment

Sungsoo Na acknowledges the financial support by the Basic Research Program of the Korea Science & Engineering Foundation, Grant No. R01-2002-000-00129-0.

Reference

(1) B. A. Boley, J. H. Weiner, 1960, "Theory of Thermal Stress", John Wiley&Sons, Inc, pp.3-355

(2) A. G. Seibert, J. S. Rice, 1973, "Coupled Thermally Induced Vibrations and Beams", AIAA Journal, Vol. 7, No. 7, pp.1033-1035.

(3) J. D. Johnson, E. A. Thornton, 1998, " Thermally Induced Attitude Dynamics of a Spacecraft with Flexible Appendage", Journal of Guidance, Control and Dynamics, Vol. 21, No. 4, pp.581-587.

(4) E. A. Thornton, Y. A. Kim, 1993, "Thermally Induced Bending Vibration of a Flexible Rolled-Up Solar Array", Journal of Spacecraft and Rockets, Vol. 30, No. 4, pp.438-448.

(5) O. Song, I. Yoon, "Thermally Induced Bending Vibration of Composite Spacecraft Booms Subjected to Solar Heating", Ph. D Thesis, Chung-Nam National University, Korea.

(6) Song, O. and Librescu, L., 1997, "Structural Modeling and Free Vibration Analysis of Rotating Composite Thin-Walled Beams", *J. of the American Helicopter Society*, Vol. 42, No. 4, pp. 358-369.

(7) Song, O., Librescu, L. Oh, S.Y., 2001, "Dynamics of Pretwisted Rotating Thin-Walled Beams Operating in a Temperature Environment", *Journal of Thermal Stresses*, Vol. 24, pp. 255-279.

(8) Na, S., and Librescu, L., 2000, "Modeling and Vibration Feedback Control of Rotating Tapered Beams Incorporating Adaptive Capabilities", *ASME 2000*, PVP-Vol. 415, Recent Advances in Solids and Structures, pp. 35-53.

(9) O. Song, "Modeling and Response Analysis of Thin-Walled Beam Structures Constructed of Advanced Composite Materials", Ph. D Thesis, VPI&SU, USA.

(10) M. Murozono, S. Sumi, 1989, "Thermally-Induced Bending Vibration of Thin-Walled Beam with Closed Section Caused by Radient Heating", Memoirs of the faculty of Engineering, Kyushu University, Vol. 49, No. 4, pp. 273-290.

(11) S. S. Na, 1997 , "Control of Dynamic Response of Thin-Walled Composite Beams Using Structural Tailing and Piezoelectric Actuation", Ph. D Thesis, VPI&SU, USA.

Appendix

Table. 1 Material and geometric properties of composite material (Graphite/Epoxy)

Parameter	Value
L	2.032 m
h	2.35E-4 m
R	0.254 m
E_1	2.068E11 N/m^2
E_2=E_3	5.171E9 N/m^2
G_{12}	3.103E9 N/m^2
G_{23}=G_{31}	2.551E9 N/m^2
μ_{12}=μ_{23}=μ_{13}	0.25
ρ	1528.227 kg/m^3
α	0.92
α_1	1.1E-6 K^{-1}
α_2	25.2E-6 K^{-1}
ε	0.84
σ	5.67E-8 W/m^{2}K^4
k	1.731 W/mK
c	1044 J/kgK
S_0	1.35E3 W/m^2